Asian Journal of Water, Environment and Pollution, Vol. 19, No. 3 (2022), pp. 1-13.
DOI 10.3233/AJW220033

Predicted Rainfall, Surface Runoff and Water Yield Responses to Climate Change in the Phetchaburi River Basin, Thailand

Ketvara Sittichok*, Jutithep Vongphet and Ousmane Seidou[1]

Irrigation Engineering Department, Faculty of Engineering at Kamphaengsaen Campus, Kasetsart University Nakhonpathom Province – 73400, Thailand

[1]Department of Civil Engineering, University of Ottawa, Ottawa, ON – K1N 6N5, Canada

✉ fengkrs@ku.ac.th

Received February 18, 2021; revised and accepted April 7, 2022

Abstract: Expected changes in temperature, rainfall, water yield and surface runoff dynamics under RCP 8.5 were estimated in the Phetchaburi River Basin, Thailand, using outputs of five regional climate models. Observed temperatures and precipitations were downscaled using a combination of quantile mapping and nearest neighbour methods. The SWAT model was used to estimate changes in hydroclimatic variables in both the near-term (2006-2050) and long-term (2051-2099) temporal frames. All models predicted higher temperatures in the future (28.7-30.4ºC) compared to the historical situation (28.0-28.3ºC). The patterns of maximum temperature from most models were shifted one month earlier but there was no significant change for minimum temperature. Disagreement between models could be found in projected precipitations for the short term, but most of them pointed to an increase in rainfall in the long term, especially for maximum rainfalls ranging from 1,637 to 1,947 mm. CNRM-CM5 presented large differences in the future rainfalls compared to other models. Surface runoff/ water yield significantly increased by 14%/17% in the long-term following the same trend as rainfalls with a slight change in the short-term.

Key words: Climate change, hydrological projections, RCPs, SWAT.

Introduction

Climate change is a pressing societal concern as it seriously threatens different dimensions of sustainability. Impacts of climate change can be seen in various domains, such as the agricultural and water resources sectors. Highly variable precipitation is apparent in equatorial regions (Dore, 2005). The effects of climate change, specifically in terms of temperature and precipitation changes, are expected to directly exacerbate stresses on crop growth and modify the length of the growing season in some areas. Precipitation decreases are likely to result in reduced water availability and lower crop productivity, whereas increasing rainfall intensity may lead to flooding. These effects of climate change put Thailand, in particular, at risk due to the main livelihood of the country which is agriculture, particularly rice cultivation.

In its Fifth Assessment Report (AR5), the Intergovernmental Panel on Climate Change (IPCC) proposed four main scenarios based on Representative Concentration Pathways (RCPs): a stringent mitigation scenario (RCP 2.6), two intermediate scenarios (RCP 4.5 and RCP 6.0), and a very high greenhouse gas (GHG) emission (RCP 8.5) scenario. The RCP metrics refer to radiative forcing values (W/m^2) expressed in a possible

*Corresponding Author

range in the year 2100 compared to pre-industrial values. According to IPCC (2014), precipitation changes under climate change scenarios will not be uniform around the world. The equatorial Pacific is likely to face an annual mean precipitation increase by the end of this century according to the RCP8.5 scenario. More intense extreme precipitation will very likely occur in tropical regions.

Due to the spatial high resolution of general circulation model outputs (GCMs), a downscaling process needs to be achieved. The two main methods of this process are dynamical and statistical downscaling. Dynamical downscaling usually refers to regional climate models (RCM) to downscale outputs of GCMs to a regional scale. The disadvantages of the projections generated using RCMs are individual-specific targets and differences in coordinating framework. Therefore, bias correction techniques or statistical downscaling methods such as, quantile mapping (QM), linear scaling and histogram equalizing are recommended or initially applied to overcome systematic modeling errors of RCM's projections (Enayati et al., 2021). QM is one of the statistical downscaling methods and is widely used in climate change areas for both rainfall and temperature variables. Trinh-Tuan et al. (2019) were able to reduce a large bias of precipitation projections in Vietnam from 45% to 3% using QM. An efficiency of this method was also presented in the work of Patel et al. (2021) presenting crucial improvement of temperature projections over India in reduction of mean uncertainty. The works of QM and their benefits for climate change research areas were also indicated in the study by Ayugi et al. (2020); Pasten-Zapata et al. (2020) and Qian and Change (2021).

Rainfall amounts and dynamics are directly related to runoff and water yields. Climate change impacts on water resources at the local scale have been extensively studied with respect to different scenarios; there is substantial spatial variability vis-à-vis which areas will likely experience increases/decreases in precipitation in the future (Usman et al., 2019). To estimate hydrological schemes, the Soil and Water Assessment Tool (SWAT) is used. SWAT is suitable for applications over extended time periods and works well with spatial information. Numerous studies have been carried out to evaluate streamflow responses under climate change scenarios using SWAT (Marhaento et al., 2018; Muhammad et al., 2020).

Even though, there were research works attempted to investigate streamflow responses to climate change (AR5) in Thailand, most works focused on the differences in GCM outputs, downscaling methods, and hydrological models with an only specific variable which was streamflow. (Ekkawatpanit et al., 2020; Gunathilake et al., 2020; Foyhirun and Promping, 2021).Therefore, the objective of this research is to investigate the dynamics of temperature, rainfall, surface runoff and water yield characteristics under climate change scenario RCP8.5 in the Phetchaburi River basin, Thailand. Downscaled temperature/rainfall measurements are utilized to consider intensity and pattern changes using the quantile mapping method whereas others were applied using the nearest-neighbour approach. The SWAT model was then used to estimate water yields and surface runoffs. Finally, the results of this research can be utilised for setting up a guideline for an adaptation plan for this area in the future.

Materials and Methods

Study Area

The Phetchaburi River basin (Figure 1) is a 6,255 km^2 watershed. The main river of the basin is the Phetchaburi River. There are 224 water resource development projects in the basin, the most important

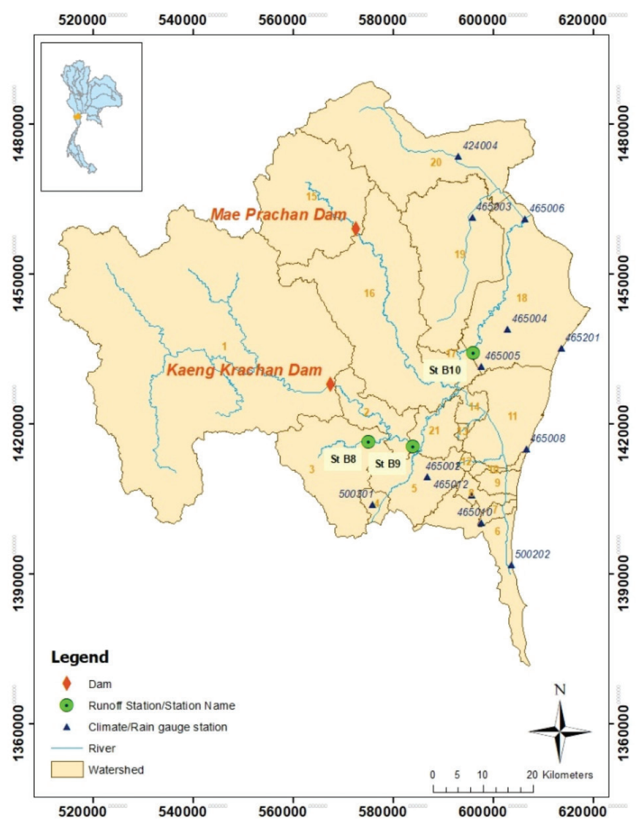

Figure 1: Climate stations, rain gauges, runoff stations and sub-watersheds in the Phetchaburi River basin.

being the Kaeng Krachan and Mae Prachan reservoirs. The mean annual precipitation is around 1,110 mm in the rainy season from May to October. The basin periodically faces both floods and droughts. Severe floods were recorded in 2016, 2017 and 2018, affecting around 197 households mainly in the lower sub-basin.

General Methodology

The general methodology is summarised in Figure 2. First, rainfall and temperature data generated by five combinations of GCMs and RCMs under RCP 8.5 were downloaded from the CORDEX website. The climate models' outputs were downscaled to the climate stations using the quantile mapping and the nearest neighbour methods. The SWAT model was then calibrated using SWAT-CUP. The dynamics of water yield and surface runoff for the entire basin were then simulated by forcing the SWAT model with downscaled rainfalls and temperatures. Comparisons between three temporal frames: 1985-2005, 2006-2050 and 2051-2099 were then described.

The SWAT Model

The SWAT was developed by the United States Department of Agriculture. It is a spatially semi-distributed hydrological model which can estimate the hydrological effects of changes in land use, management practices, and climate on water amount and sediment yield (Neitsch et al., 2011). Input data required for SWAT fall into two categories: time series and spatial data. The time series data set comprises rainfall, minimum and maximum temperature, relative humidity, radiation, wind speed and dam release. DEM, soil group and land use maps including the locations and characteristics of dams were forced to the model. In the model, a watershed is divided into sub-watersheds and further partitioned into HRUs, which are functions of soil, land use, and slope.

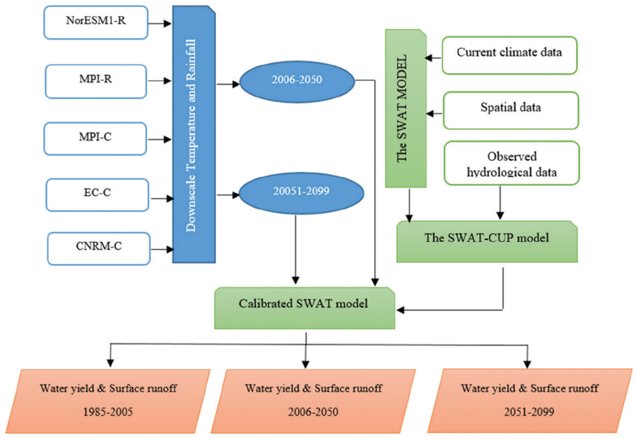

Figure 2: Methodology flowchart.

Data Preparation

Observed Climate Time Series

Rainfall data from nine rain gauge stations inside and around the basin were prepared by the Thai Meteorological Department for 31 years (1985-2015). Data of other climatic factors such as minimum-maximum temperature, relative humidity, wind speed, and sunshine hours were collected on a daily basis from two main climate stations. Monthly hydrological records spanning 1999-2015 at four stations were collected from the Royal Irrigation Department including daily water releases from reservoirs.

RCM Outputs

Daily precipitation and minimum-maximum temperature from five climate experiments (combination of GCMs and RCMs) were used in this study. Five GCMs and two RCMs were employed (Table 1). The outputs of these models were studied in various research works where it was found that they have an excellent performance. MPI-ESM-LR was found to be one of the six top models for precipitation simulation in Asia among 37 global

Table 1: The details of GCM-RCM combination

Abbreviation	*Institution*	*GCM*	*Spatial resolution of GCM*	*RCM*	*Spatial resolution of RCM (degree)*
NorESM-R	Norwegian Climate Centre	NorESM1-M	2.5×1.9	REMO2015	0.11
MPI-R	Max Planck Institute for Meteorology	MPI-ESM	1.9×1.9	REMO2015	0.11
MPI-C				CCLM5-0-2	0.44
EC-C	EC-EARTH consortium, the Netherlands/Ireland	EC-EARTH	1.1×1.1	CCLM5-0-2	0.44
CNRM-C	Météo-France/Centre National de Recherches Météorologiques	CNRM-CM5	1.4×1.4	CCLM5-0-2	0.44

climate models (Ta et al., 2018). Aflahah et al. (2019) found that precipitation generated using NorESM1-M presented a high correlation with observation in Indonesia and Southeast Asia. NorESM1-M also showed good performance for maximum temperature simulations (Panjwani et al., 2019). Jia et al. (2019) compared 33 GCMs for East Asia and found that EC-EARTH was one of three models that performed well in simulating mean rainfall. EC-EARTH and CNRM-5 was also selected for use in Southeast Asia (Tangang et al., 2018, 2020).

Statistical Downscaling

Projected precipitations and minimum-maximum temperatures were downscaled using quantile mapping bias correction which was widely used for downscaling (Luo et al., 2018; Mendez et al., 2020). The quantile mapping method is a non-parametric bias correction and can be applied for most possible distributions. The bias in the mean, standard deviation, wet–dry frequency can be corrected using this method. For both precipitation and temperature, their adjustment can be described in terms of their empirical cumulative distribution function (*ecdf*) and it is inverse presented in Equation 1. The quantile mapping method can express the data in terms of *ecdf* and its inverse ($ecdf^{-1}$). $P/T_{raw,m,d}$ refers to the raw precipitation/temperature on the *d*th day of *m*th month. $ecdf_{raw,m}$ and $ecdf^{-1}_{o,b,s,m}$ represents *ecdf* of raw precipitation and temperature data of *m*th month and its inverse of observed data of *m*th month. Finally, corrected precipitation and temperature ($P/T_{cor,m,d}$) were calculated.

$$P/T_{cor,m,d} = ecdf^{-1}_{o,b,s,m}(ecdf_{raw,m}(P/T_{raw,m,d})) \quad (1)$$

Future values of relative humidity (HMD), wind speed (WND), and solar radiation (SLR) were downscaled by using the nearest-neighbour approach: For each day in the future period (*df*), one day is chosen from the historical period from the same month (*dh*), and the absolute difference between the closest average temperature of *df* and *dh* is minimal. The HMD, SLR, and HMD of *dh* are then assigned to *df*.

Results

SWAT Model Calibration for the Phetchaburi River Basin

Model calibration was performed using SWAT-CUP and the five most sensitive parameters for this basin are presented in Table 2. Across all stations, there was good agreement between observation and prediction: R^2 = 0.45-0.71, NSE = 0.37-0.70 and Pbias = -16 - +35%. Simulated streamflows were generally able to capture low to average flows but had difficulties in reaching some peak events such as at station B10 in October 2013 because of measuring stations located close to the diversion dam (Figure 3).

The hydrological cycle of this basin was also revealed. The average rainfall of the basin generally was recorded to be 5,928 mcm/year. Evapotranspiration occurred around 2,281 mcm/year (38% of the rainfall). Rainfall was recharged to groundwater of 2,738 mcm/year (46% of the rainfall) and converted to runoff around 910 mcm/year (15% of the rainfall). Changing both rainfall amount and its pattern definitely affects this cycle. The higher or lower amount of rainfall was related to soil water content leading to infiltration rate in soil resulting in the change of groundwater and surface runoff.

Temperature Changes Under RCP8.5

The basin was expected to face a warmer climate under RCP 8.5. Figure 4 and Table 3 show the changes in mean annual temperature. During the historical period, the average temperature was in the range of 28.0-28.3ºC, whereas during the near-term and long-term periods it increased to 28.7-29.1ºC and 29.7ºC-30.4ºC. It can be noticed that the MPI-C model presented the highest

Table 2: Suitable range of fivemost sensitive parameters of Phetchaburi River basin

Parameter Name		*Unit*	*Range*	*Default Range*
			Min-Max	
CN2.mgt	Initial SCS runoff curve number for moisture condition II	-	35.24-89	35-98
ALPHA_BF.gw	Base flow alpha factor	-	0.001-0.84	0-1
CH_N2.rte	Manning’s N value for the main channel	-	0.014-0.029	0-0.3
CH_N1.sub	Manning’s N value for the tributary channel	-	0.014-0.029	0-0.3
ESCO.hru	Soil evaporation compensation factor	-	0.15-0.96	0-1

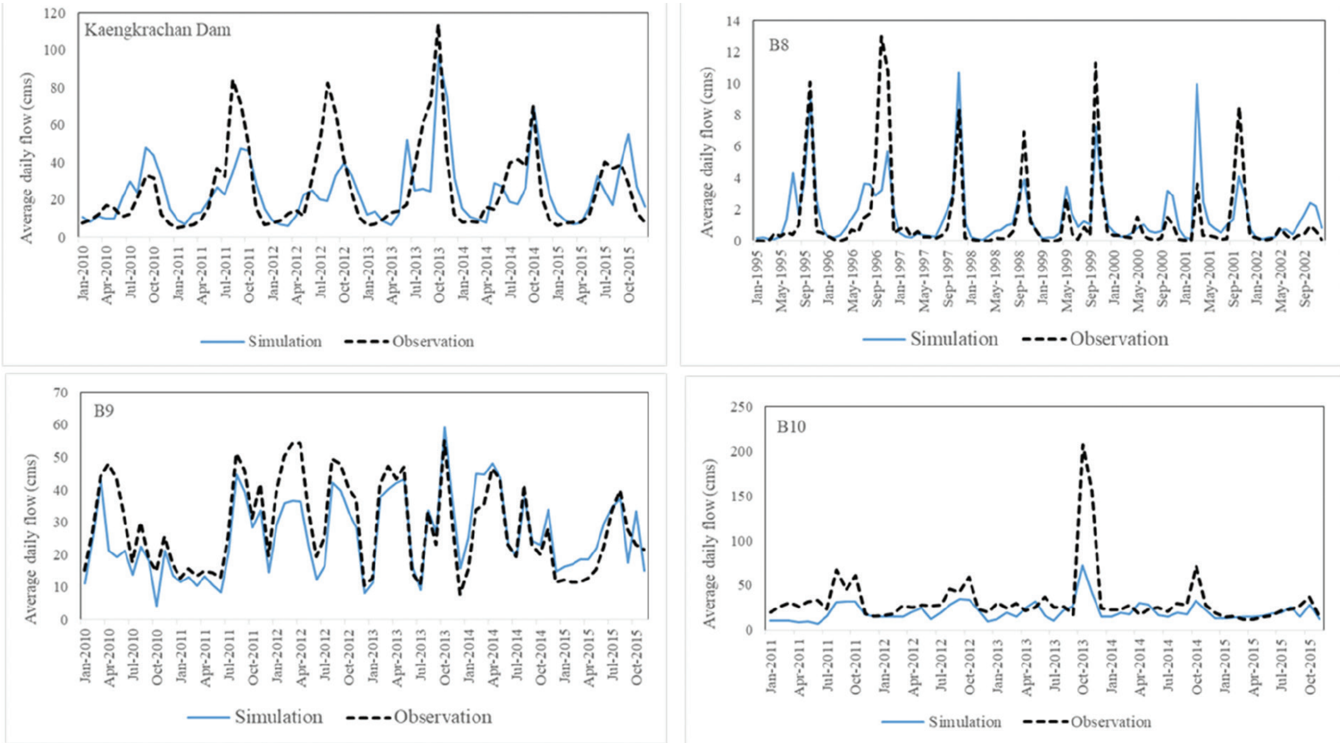

Figure 3: Comparison between observation and simulation for calibration process.

Table 3: Average annual temperature during historical, near-term and long-term periods

	NorESM-R	*MPI-R*	*EC-C*	*MPI-C*	*CNRM-C*	*Avg. Temperature*
ST 465201						
1985-2005	28.2	28.2	28.0	28.2	28.2	28.1
2006-2050	28.7	28.7	28.9	29.0	28.8	28.9
2051-2099	29.7	30.2	30.3	30.4	30.0	30.3
ST 500202						
1985-2005	28.3	28.2	28.2	28.3	28.3	28.3
2006-2050	28.6	28.8	29.0	29.1	28.6	29.0
2051-2099	29.7	30.1	30.2	30.3	30.1	30.3

temperature. Unsurprisingly, all models presented a trend that climbed up until the end of the century. The variability of annual temperature also increased with time. In the past, the standard deviation of annual temperature was in the range of 0.2-0.3ºC. They increased substantially for both stations in the near-term (0.3-0.4ºC) and the long-term (0.4-0.7ºC).

Monthly temperatures (Figure 5) were also considered since their changes are related to evapotranspiration that could point to agricultural water consumption used for crop planning in the future. Simulations of maximum monthly temperature usually occurred in May during 1985-2005. In the future for ST 465201, the month of maximum temperature in NorESM-R, MPI-R and CNRM-C simulations shifted from May to April. Opposite results were obtained with EC-C and MPI-C for which the highest temperatures were recorded a few months later. The same changes were observed at ST 500202 except for CNRM-C, for which no change in the month of maximum temperature was observed. The minimum temperature normally took place from December to January. The date of the lowest temperature in the year shifted to one month earlier for both terms except for MPI-C. The impact of climate change on monthly temperatures could be clearly seen during the summer and rainy seasons, especially in the long-term.

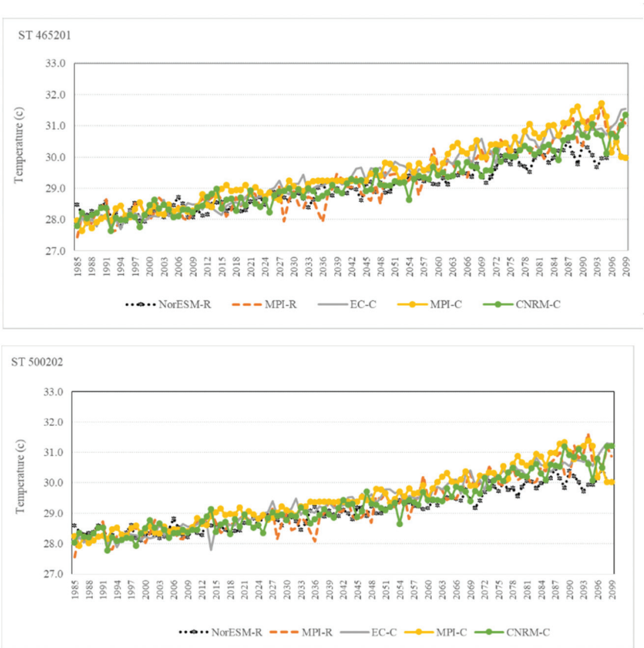

Figure 4: Annual temperature under climate change scenarios.

Rainfall Changes Under RCP8.5

The projected changes in annual rainfall are presented in Figure 6 as a percentage of annual rainfall during the reference period. For the near-term, NorESM-R, EC-C and CNRM-C projected rainfall reduction in the range of -30.9 to -3.9%. The largest rainfall decrease for all stations was obtained with CNRM-C. Another two models – MPI-R and MPI-C provided opposite results with rainfall increments in the range of 1.7-28.0%. The greatest increases in rainfall were predicted by MPI-C. All models projected an increase of rainfall in the long term in the range of 2.7-33.2% except CNRM-C. The greatest reduction/increment was projected by CNRM-C/MPI-R for both terms. Figure 7 shows an areal average of annual rainfall projections for the basin calculated using the Thiessen polygon method. The average rainfall amounts of all models during 1985-2005 were 1,119 mm, while the near- /long- term presented average rainfalls of 1,093/1,181 mm. The lowest and largest rainfalls of the near-term were 917 and 1,281 mm projected by CNRM-C and MPI-C, respectively. A severe rainfall shortage developed by all models occurred in 2046 (675 mm). The long-term period gave the lowest/largest average rainfalls of 838 and 1,337 mm developed by CNRM-C and EC-C.

Large variations of monthly rainfalls are shown in Figure 8. Monthly projected rainfalls averaged from all models mostly decreased in the near-term during the wet season. Increasing rainfall projection in the long-term noticeably indicated at the beginning of the wet period and slightly reduced at the end of the season. All models presented a higher amount of rainfall for both periods in June-August except CNRM-C.

Water Yields and Surface Runoffs Under RCP 8.5

As expected given rainfall projections, water yields and runoffs in future periods significantly changed. Projected annual water yields and surface runoffs generated using each model are presented in Table 4. For the near-term, NorESM-R, EC-C and CNRM-C projected a decrease in water yield and runoff, consistent with their projections of a reduction in rainfall. According to these three models, water yields and surface runoffs were expected to be reduced by around –25.6% to –3.2% and –24.5% to –4.5% compared to the current situation. On the other hand, MPI-R and MPI-C showed an increase of 20.0% -23.9% and 21.7%-23.3% for water yields and surface runoffs, respectively. However, all models agreed with the increment of both variables for the long term with the range between 18.9%-47.7% and 23.7%-53.0% except CNRM-C. Details of water yield and surface runoff amounts of all models are presented in Table 4 and Figure 9.

Monthly surface runoffs and water yields are plotted in Figure 10. These variables were also taken into consideration since they are significant to agricultural

Table 4: The amount of water yield and surface runoff of the basin

	1985-2005		*2006-2050*		*2051-2099*	
	Water yield (mm)	*Surface runoff (mm)*	*Water yield (mm)*	*Surface runoff (mm)*	*Water yield (mm)*	*Surface runoff (mm)*
NorESM-R	10,391	6,688	10,059 (-3.2%)	6,314 (-5.6%)	15,356 (47.7%)	10,235 (53.0%)
MPI-R	9,702	6,194	11,647 (20.0%)	7,536 (21.7%)	11,858 (22.2%)	7,887 (27.3%)
EC-C	14,020	9,721	12,870 (-8.2%)	9,288 (-4.5%)	16,674 (18.9%)	12,375 (27.3)
MPI-C	13,207	9,265	16,368 (23.9%)	11,428 (23.3%)	16,812 (27.3%)	11,460 (23.7%)
CNRM-C	14,673	10,456	10,915 (-25.6%)	7,930 (-24.5%)	10,022 (-31.7%)	7,658 (-26.8%)

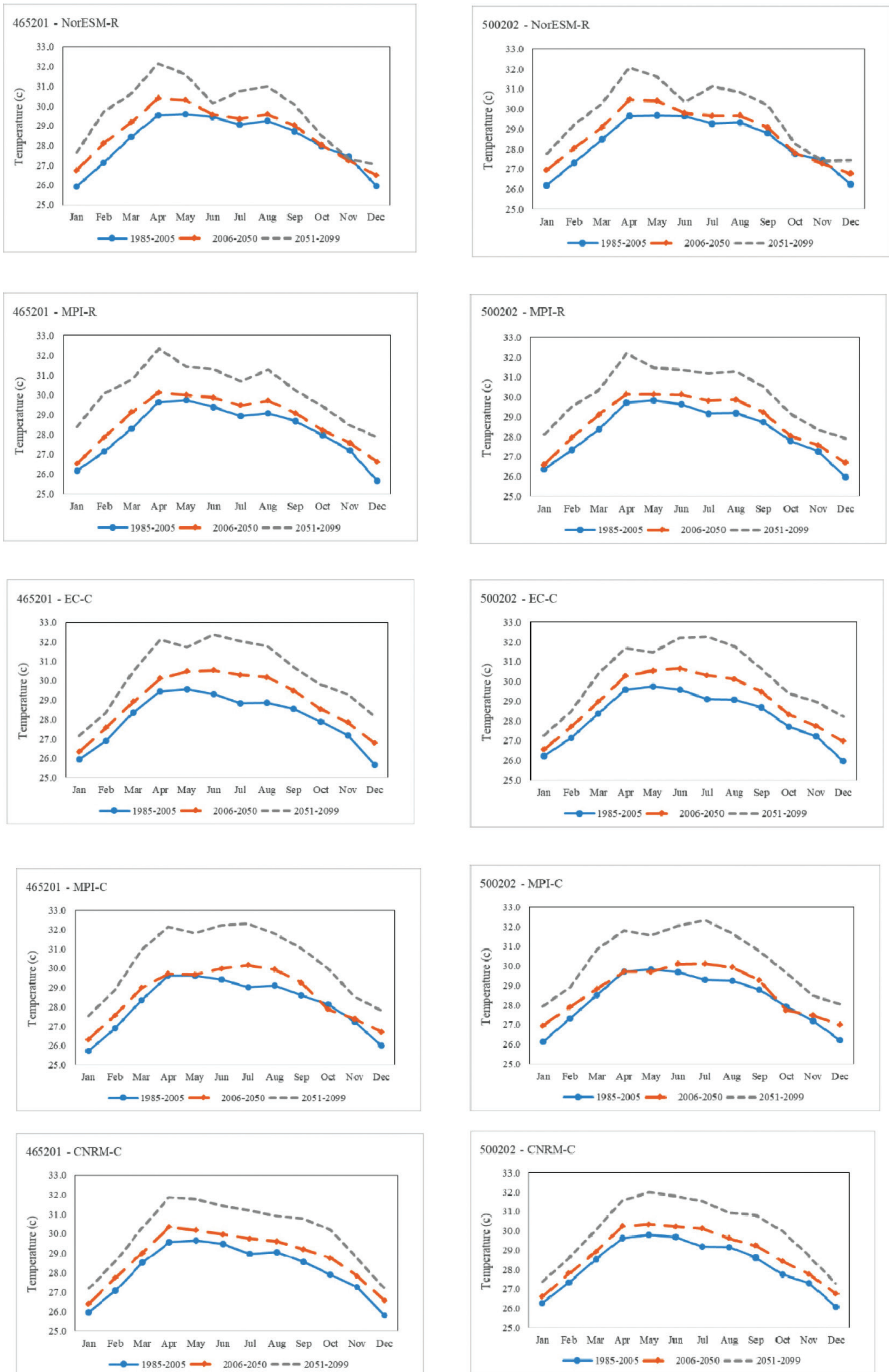

Figure 5: Multi-models average monthly temperature under climate change scenarios.

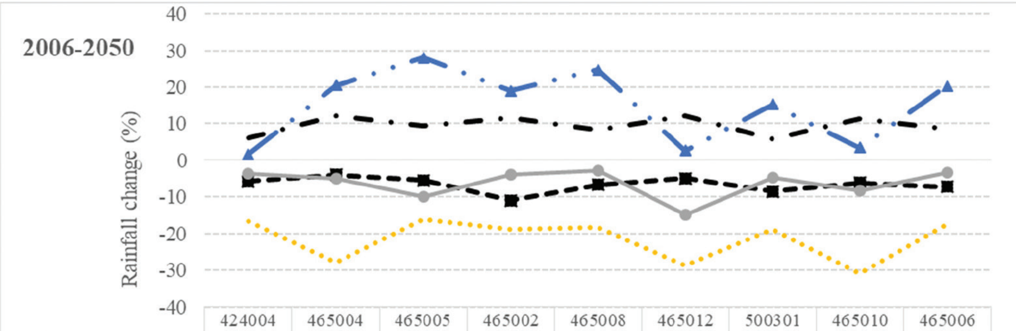

	424004	465004	465005	465002	465008	465012	500301	465010	465006
NorESM-R	-5.7	-3.9	-5.4	-11.0	-6.7	-4.9	-8.4	-6.2	-7.2
MPI-R	6.2	12.3	9.3	11.7	8.4	12.3	5.9	11.4	8.6
EC-C	-3.6	-5.0	-9.8	-3.9	-2.8	-14.8	-4.6	-8.3	-3.3
MPI-C	1.7	20.4	28.0	19.0	24.7	2.6	15.3	3.4	20.4
CNRM-C	-16.7	-27.9	-16.2	-18.9	-18.3	-28.8	-18.8	-30.9	-17.5

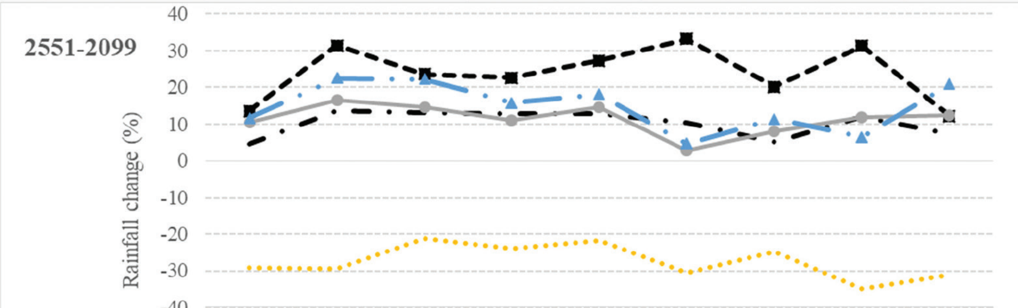

	424004	465004	465005	465002	465008	465012	500301	465010	465006
NorESM-R	13.5	31.4	23.6	22.7	27.3	33.2	20.1	31.3	12.1
MPI-R	4.6	13.6	13.1	12.9	12.9	10.4	5.1	12.1	7.3
EC-C	10.4	16.4	14.7	11.0	14.5	2.7	8.0	11.7	12.4
MPI-C	11.6	22.5	22.2	15.8	18.1	4.6	11.4	6.5	20.9
CNRM-C	-29.1	-29.6	-21.2	-24.1	-21.8	-30.5	-24.7	-34.8	-31.2

Figure 6: Rainfall changes under climate change scenarios: the near-term (above) and the long-term (below).

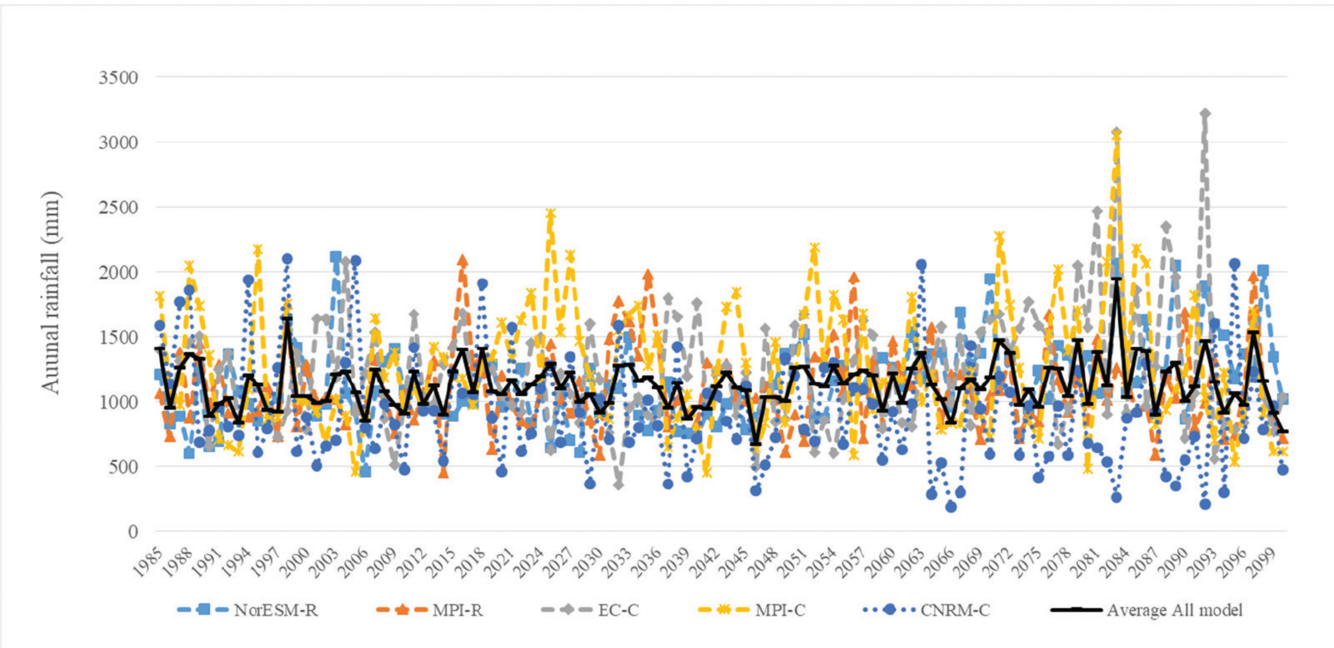

Figure 7: Annual rainfall changes for all stations.

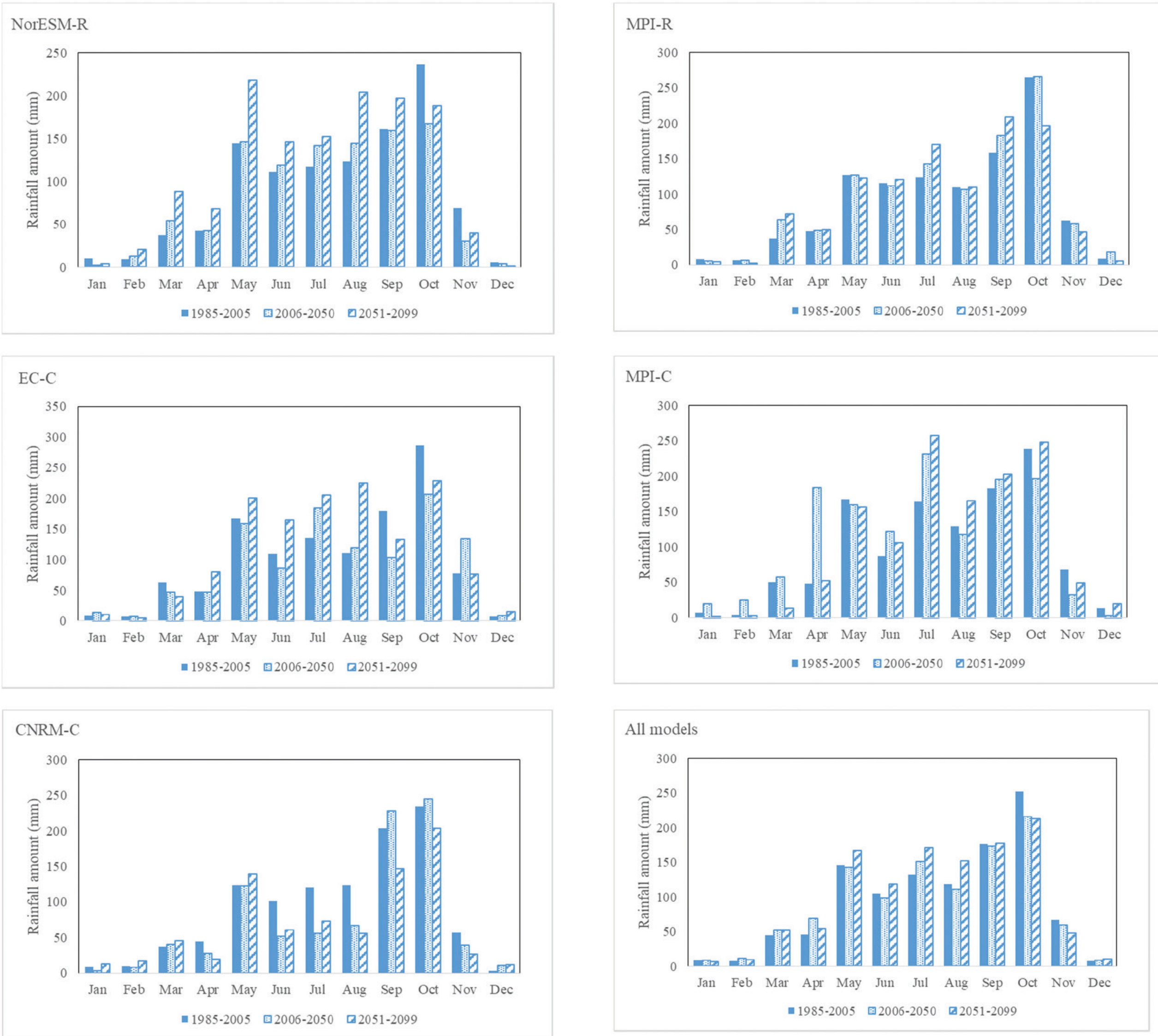

Figure 8: Average monthly rainfall projections.

plans, dam operation and decision policy. The maximum water yields and surface runoff occurred in October for both periods of all models. However, there was a slight variation between models. A higher amount of water yield and surface runoff during the wet period could be seen for all models with variation for each month except CNRM-C giving a lower amount. The lowest surface runoff and water yields still remained in February (the dry season). Decreasing water yields and surface runoffs occurred during the dry season could be seen in NorESM-R and EC-C.

Discussions

All models strongly agreed with an increment of temperature around 1°C at the end of the near-term and 2°C in 2099. However, a contradiction between models could be seen in the projections of precipitation due to more complexity in a natural process compared to temperature. CNRM-C showed the largest decrease of projected rainfalls during 2551-2099, which disagreed with other models presenting significant increments. The inconsistency between models could be found in the projected precipitation during 2006-2050. CNRM-C still generated a large rainfall reduction in this period which was substantially different from others. The peak value of average rainfalls still generally occurred in October with slightly less than the historical situation, but higher average rainfall projections were obviously seen during the wet season. Average rainfall projections at the monthly time scale tended to be higher compared

Figure 9: Annual water yield (Left) and surface runoff (Right) of the entire basin for all five models.

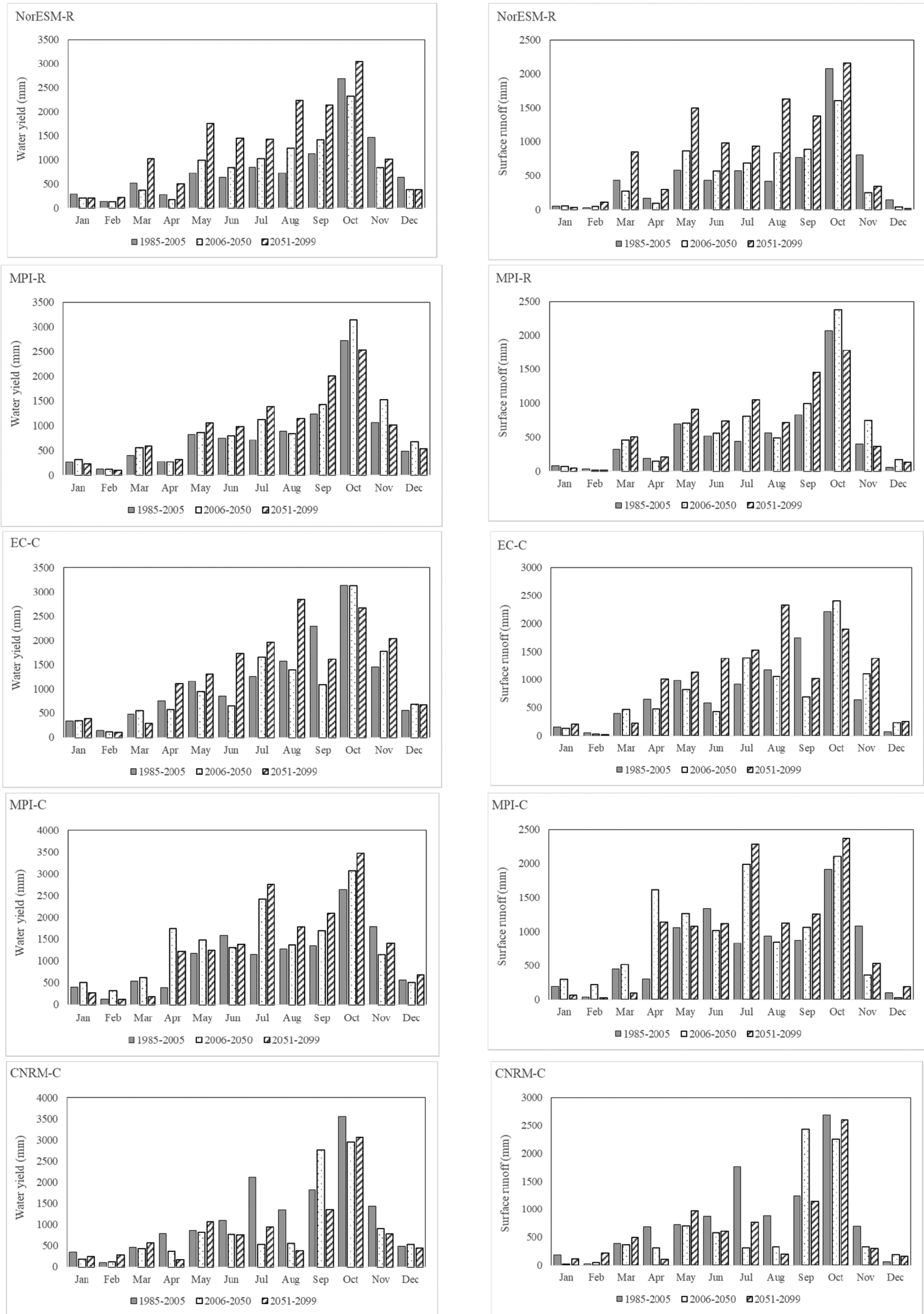

Figure 10: Monthly water yields (Left) and surface runoffs (Right) of the entire basin for all five model.

to the historical, especially at the beginning of the rainy season.

The results of annual and monthly runoffs and water yields were strongly corresponding to projected rainfalls as expected. The frequencies of higher annual runoff and water yield occurrences compared to the average tended to be larger in the future for both periods. Average results of both projected hydrological variables at the beginning of a wet season were higher/lower than the historical period at the beginning of the wet/dry season. The changes in rainfalls, water yields and runoffs, in both annual and monthly time scale, lead to an awareness of irrigation and water management adjustment under climate change situation in the near future.

Conclusions

Scientific knowledge and information about climate change impacts on hydrological variables are crucial for informing policy responses to mitigate and/or adapt to extreme events and other outcomes. Peak runoff and water yield for the basin are important concerns vis-à-vis climate change preparedness. This research estimated changes in rainfall, water yield and surface runoff in the Phetchaburi River Basin, Thailand for two periods: 2006-2050 (the near-term) and 2051-2099 (the long-term) under RCP 8.5 climate change scenarios. The quantile mapping method was employed in this study for statistical downscaling of RCM outputs prepared by CORDEX. The SWAT model initially calibrated using the SWAT-CUP program was beneficial for the projections of runoff and water yield. This research mainly found that temperatures and rainfalls averaged from all models increases steadily in the future periods under climate change scenarios compared to the historical period. Disagreement among models could be indicated only in projected rainfalls for the near-term. Projected average water yields and surface runoffs were also increased corresponding to future rainfalls. The selection of GCM output for hydrological study in a specific area should be carefully considered due to the large difference in their results.

Acknowledgements

This research was funded by the Agricultural Research Development Agency (ARDA), Thailand.

References

Aflahah, E., Latifah, A.L., Hidayat, R., Hidayati, R. and A. Ihwan (2019). Inter-comparison of multiple global climate model (GCM) data based on spatial pattern of rainfall over Indonesia. *Conf. Series: Earth and Environmental Science*, **284(1):** 012017.

Ayugi, B., Tan, G., Ruoyun, N., Babaousmail, H., Ojara, M., Wido, H., Mumo, L., Ngoma, N.H., Noono, I.K. and V. Ongoma (2020). Quantile mapping bias correction on Rossy Centre regional climate models for precipitation analysis over Kenya, East Africa. *Water*, **12:** 801.

Dore, M.H.I. (2005). Climate change and changes in global precipitation patterns: What do we know?. *Environmental International*, **31:** 1167-1181.

Ekkawatpanit, C., Pratoomchai, W., Khemngoen, C. and P. Srivihok (2020). Climate change impact on water resources in Klong Yai River Basin, Thailand. *Proceeding of the International Association of Hydrological Sciences*, **383:** 355-365.

Enayati, M., Bozorg-Haddad, O., Bazrafshan, J., Hejabi, S. and X. Chu (2021). Bias correction capabilities of quantile mapping methods for rainfall and temperature variables. *Journal of Water and Climate Change*, **12(2):** 401-419.

Foyhirun, C. and T. Promping (2021). Future hydrological drought hazard assessment under climate and land use projections in Upper Nan River Basin, Thailand. *Engineering and Applied Science Research*, **48(6):** 781-790.

Gunathilake, M.B., Amaratunga, Y.V., Perera, A., Chathuranika, I.M., Gunathilake, A.S. and U. Rathnayake (2020). Evaluation of future climate and potential impact on streamflow in the upper Nan River Basin of Northern Thailand. *Advances in Meteorology*, **2020:** 8881118.

IPCC (2014). Climate Change 2014: Synthesis Report. Contribution of Working Groups I, II and III to the Fifth Assessment Report of the Intergovernmental Panel on Climate Change [Core Writing Team, R.K. Pachauri and L.A. Meyer (eds.)]. IPCC, Geneva, Switzerland, 151pp.

Jia, K., Ruan, Y., Yang, Y. and C. Zhang (2019). Assessing the performance of CIMP5 global climate models for simulating future precipitation change in the Tibetan Plateau. *Water*, **11(1771):** 1-18.

Luo, M., Liu, T., Meng, F., Duan, Y., Frankl, A., Bao, A. and P.D. Maeyer (2018). Comparing bias correction methods used in downscaling precipitation and temperature from regional climate models: A case study from the Kaidu River Basin in Western China. *Water*, **10(8):** 1046.

Marhaento, H., Booji, M.J. and A.Y. Hoekstra (2018). Hydrological response to future land-use change and climate change in a tropical catchment. *Hydrological Science Journal*, **63(9):** 1368-1385.

Mendez, M., Maathuis, B., Hein-Griggs, D. and L. Alvarado-Gamboa (2020). Performance evaluation of bias correction methods for climate change monthly precipitation projections over Costa Rica. *Water*, **12(2):** 482.

Muhammad, A., Evenson, G.R., Unduche, F. and T.A Standnyk (2020). Climate change impacts on reservoir inflow in the Prairie Pothole region: A watershed model analysis. *Water*, **12(1):** 271.

Neitsch, S.L., Arnold, J.G., Kiniry, J.R. and J.R. Williams (2011). Soil and Water Assessment Tool Theoretical Documentation version 2009. *In:* Texas Water Resources Institute Technical Report No. 406. Texas A&M University System, College Station, Texas.

Panjwani, S., Naresh Kumar, S., Ahuja, L. and A. Islam (2019). Prioritization of global climate models using fuzzy analytic hierarchy process and reliability index. *Theoretical and Applied Climatology*, **137:** 2381-2392.

Pasten-Zapata, E., Jones, J.M., Moggridge, H. and M. Widmann (2020). Evaluation of the performance of Euro-Cordex regional climate models for assessing hydrological climate change impacts in Great Britain: A comparison of different spatial resolutions and quantile mapping bias correction methods. *Journal of Hydrology*, **584:** 124653.

Patel, J., Ghanaseelan, C., Chowdary, J.S. and A. Parekh (2021). A quantile mapping approaches-based bias correction in coupled model intercomparison project phase 5 models for decadal temperature predictions over India. *International Journal of Climatology*, **42(4):** 2455-2469.

Qian, W. and H.H. Chang (2021). Projecting health impacts of future temperature: a comparison of quantile-mapping bias correction methods. *International Journal of Environmental Research and Public Health*, **18(4):** 1992.

Tangang, F. et al. (2020). Projected future change in rainfall in Southeast Asia based on Cordex-SEA multi-model simulations. *Climate Dynamics*, **55:** 1247-1267.

Tangang, F., Supari, S., Chung, J.X. Cruz, F., Salimun, E., Ngai, S.T., Juneng, L., Santisirisomboon, J., Ngo-Duc, T., Phan-van, T., Narisma, G., Singhruck, P., Gunawan, D., Aldrian, E., Sopaheluwakan, A., Nikulin, G., Yang, H., Remedio, A.R., Sein, D. and D. Hein-Griggs (2018). Future changes in annual precipitation extremes over Southeast Asia under global warming of 2ºC. *APN Science Bulletin*, **8(1):** 3-8.

Ta, Z., Yu, Y., Sun, L., Chen, X., Mu, G. and R. Yu (2018). Assessment of precipitation simulations in central Asia by CMIP5 Models. *Water*, **10(11):** 1516.

Trinh-Tuan, L., Matsumoto, J., Tangang, F.T., Juneng, L., Cruz, F., Narisma, G., Santisirisomboon, J., Phan-Van, T., Gunawan, D., Aldrian, E. and T. Ngo-Duc (2019). Application of quantile mapping bias correction for mid-future precipitation projections over Vietnam. *SOLA,* **15:** 1-6.

Usman, M., Ahmad, B. and S.A.A. Bukhari (2019). Assessment of inter-seasonal, inter-annual and intra-annual variability in snow and rainfall recharged fresh water discharge under IPCC AR5 based climate change scenarios: A case study of Soan river basin, Potowar region, Pakistan. *Climate Change*, **5(20):** 264-326.

Asian Journal of Water, Environment and Pollution
Volume 18 Number 1 **January – March, 2021**

Contents